Determination of the magnetic ground state of a polycrystalline compound based on susceptibility measurements

Randy S. Fishman[1] and Joel S. Miller[2]

[1]*Materials Science and Technology Division, Oak Ridge National Laboratory, Oak Ridge, Tennessee 37831-6453, USA*

[2]*Department of Chemistry, University of Utah, Salt Lake City, Utah 84112-0850, USA*

(Received 22 November 2010; revised manuscript received 26 January 2011; published 30 March 2011)

The diruthenium compound $[Ru_2(O_2CMe)_4]_3[Cr(CN)_6]$ contains two interpenetrating sublattices that behave like giant antiferromagnetically coupled moments with strong anisotropy. Preferred orientations of the total moment of each sublattice are determined from susceptibility measurements on a polycrystalline sample. In agreement with previous predictions, fits to the experimental magnetization indicate that the sublattice moments are aligned along cubic diagonals rather than cubic axis or edge diagonals. The parametrization of the sublattice susceptibility implies that the sublattice spin states are more deformed when aligned antiparallel.

DOI: 10.1103/PhysRevB.83.094433 PACS number(s): 75.50.Xx, 75.10.Dg, 75.30.Gw

I. INTRODUCTION

Diruthenium tetracarboxylate, $[Ru_2(O_2CMe)_4]_3$ $[Cr(CN)_6]$ (*Me* = methyl, CH_3),[1–4] or $Cr(Ru_2)_3$ for short, may be the only known compound where two weakly interacting, magnetically ordered sublattices occupy the same three-dimensional volume. Antiferromagnetically (AF) coupled sublattices[5,6] become aligned above the critical field $H_c \sim 1000$ Oe and below the critical temperature $T_c \approx 33$ K.[7] Based on a simple model for the metamagnetic transition, a great deal of useful information can be extracted from the average magnetization $2\mu_B M_{av}(T,H)$ of a polycrystalline $Cr(Ru_2)_3$ sample. In particular, the average magnetization can be used to determine the anisotropy axis of the individual sublattices.

A single sublattice of $Cr(Ru_2)_3$, sketched in the inset of Fig. 1, has a cubic unit cell with dimension $a_l = 13.4$ Å. The $[Cr(CN)_6]^{3-}$ (called Cr for short) ions on the corners of the cube are separated by Ru_2 complexes. A second identical sublattice fills the open space of the first sublattice to produce a body-centered-cubic structure.

Magnetically, each Ru_2 complex is in a delocalized, mixed-valent (II/III) state with total spin $S = 3/2$.[1] Due to the "paddle-wheel" molecular environment produced by the surrounding four *Me* groups, each Ru_2 spin **S** experiences easy-plane anisotropy $D(\mathbf{S}\cdot\mathbf{v})^2$, with $D \approx 100$ K or 8.6 meV,[8,9] and unit vector **v** pointing to one of the neighboring Cr ions. Because the two sublattices have very weak molecular overlap, the AF coupling $J_c \sim 5\times10^{-3}$ meV between sublattices is much weaker than the AF coupling $J_c \sim 1.5$ meV within each sublattice between a $S = 3/2$ Ru_2 (II/III) complex and the two neighboring $S = 3/2$ Cr (III) ions.

Of course, the best way to resolve the magnetic ground of a molecule-based material is by performing elastic neutron-scattering measurements on a deuterated single crystal. For an anisotropic material, magnetization measurements on a single crystal can determine the easy and hard axis. However, single crystals of molecule-based compounds are often impossible to synthesize and deuteration is quite expensive. So it is important to extract as much information as possible from available polycrystalline samples.

For fields far below $J_cS/\mu_B \sim 25$ T and $DS/\mu_B \sim 200$ T, the internal structure of each sublattice is nearly rigid and each sublattice spin $M_{sl}\mathbf{n}_i$ (i = 1 or 2) is confined by anisotropy barriers to certain high-symmetry orientations. We use the average magnetization of polycrystalline $Cr(Ru_2)_3$ to determine the possible orientations $\mathbf{n}_i$ of the sublattices in small fields. In agreement with earlier work,[5] the best fits to the experimental data are obtained when $\mathbf{n}_i$ are restricted to the cubic diagonals. A more sophisticated parametrization of the sublattice susceptibility indicates that the sublattice states are more deformed when aligned antiparallel.

Section II below summarizes previous results for the ground state of a single sublattice of $Cr(Ru_2)_3$ and Sec. III presents a simple model for the metamagnetic transition. Section IV analyzes the fits to the experimental data at ambient pressure under one of three possible conditions: $\mathbf{n}_i$ restricted (i) to cubic diagonals like (111), (ii) cubic axis like (100), or (iii) edge diagonals like (110). We also present results for the fitting parameters under case (i). The pressure dependence of the fitting parameters discussed in Sec. V provides dramatic evidence for a low-pressure (LP) to high-pressure (HP) phase transition at about 7 kbar and supports our earlier conjecture of a high- to low-spin transition on the Ru_2 complexes.[6] A brief summary is provided in Sec. VI.

II. MAGNETIC GROUND STATE

In the inset to Fig. 1, Ru_2 pairs are labeled as a (along the x axis), b (along y), or c (along z). For classical spins with infinite anisotropy, the a, b, or c spins must lie on the yz, xz, or xy planes, respectively. Quantum spins will have small components in the classically forbidden directions.[5] If the total Ru_2 spin on the a, b, and c sites lies along the (111) direction, the directions of the individual a, b, or c spins are given by (u,w,w), (w,u,w), or (w,w,u) with $u^2 + 2w^2 = 1$. For classical spins, $u \to 0$ as $D \to \infty$. Because anisotropy is absent on the Cr sites, the Cr spins are predicted to point opposite the net Ru_2 spin along one of the eight cubic diagonals.

For classical spins with infinite anisotropy, the net sublattice spin along a cubic diagonal at $T = 0$ is

$$M_{sl} = (\sqrt{6} - 1)S \approx 1.45S \tag{1}$$

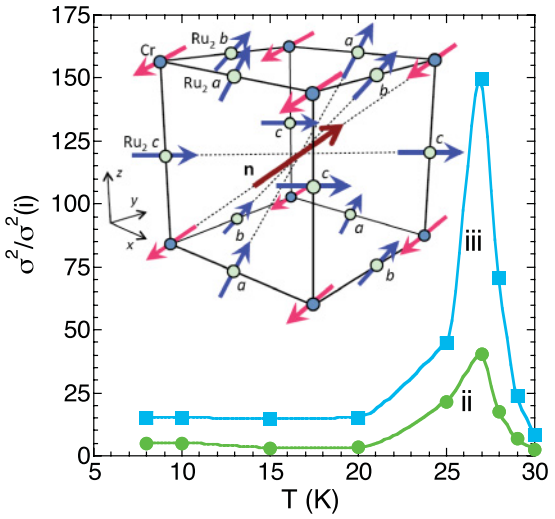

FIG. 1. (Color online) Inset is the predicted ground state of a single sublattice of $Cr(Ru_2)_3$ for infinite anisotropy and classical spins. The net sublattice spin is oriented along the $\mathbf{n} \propto (111)$ direction antiparallel to the Cr spins (corresponding to case i). Ratios of $\sigma^2/\sigma^2(i)$ are plotted versus temperature for cases (ii) and (iii).

per Cr ion. For quantum spins with finite anisotropy, the net spin at any temperature is

$$M_{\rm sl} = \sqrt{3} M_{\rm Ru_2}(\sqrt{2(1-u^2)} + |u|) - M_{Cr}. \qquad (2)$$

In either case, the net sublattice spin is opposite to the Cr spin and parallel to the total Ru_2 spin on the a, b, and c sites. Due to the tilt of the Ru_2 spins away from their easy planes, the amplitude of the Ru_2 spin $M_{\rm Ru_2}$ is suppressed from 3/2 even at $T = 0$.

III. MODEL FOR THE METAMAGNETIC TRANSITION

At $T = 0$ and $H < H_c$, the two sublattices are AF aligned with $\mathbf{n}_1 = -\mathbf{n}_2$. At $T = 0$ and $H > H_c$, the sublattice orientations $\mathbf{n}_1 = \mathbf{n}_2$ in the paramagnetic (PM) state lie along the anisotropy axis that is closest to the field direction $\mathbf{m}$. The analysis summarized in the previous section suggests that the anisotropy axes are the eight cubic diagonals. At a nonzero temperature, thermal equilibrium between the 64 possible configurations of $\{\mathbf{n}_1,\mathbf{n}_2\}$ is then achieved by fluctuations out of the ordered AF or PM state.

We now generalize the earlier model for the metamagnetic transition by allowing the sublattice spin to be oriented either (i) along cubic diagonals like (111), (ii) along cubic axis like (100), or (iii) along edge diagonals like (110). For any of these three cases, the energy of a magnetic configuration with sublattice orientations $\{\mathbf{n}_{1i},\mathbf{n}_{2i}\}$ on cluster i is given by

$$E = N_{\rm Cr} \sum_i \{ -\mu_B M_{\rm sl}(\mathbf{n}_{1i} + \mathbf{n}_{2i}) \cdot \mathbf{H} + K_c {M_{\rm sl}}^2 \mathbf{n}_{1i} \cdot \mathbf{n}_{2i} \}, \qquad (3)$$

where $\mathbf{H} = H\mathbf{m}$ is the magnetic field and there are 64, 36, or 144 possible configurations for $\{\mathbf{n}_{1i},\mathbf{n}_{2i}\}$. Each cluster i contains $N_{\rm Cr} \propto \xi^3$ $Cr(Ru_2)_3$ unit cells, half belonging to each sublattice. The correlation length ξ decreases as magnetic fluctuations are suppressed.

In order to account for the small deformation of each sublattice ground state in a weak magnetic field, we previously introduced the susceptibility $\chi_{\rm sl} \equiv 2\mu_B d(\mathbf{M}_{\rm sl} \cdot \mathbf{m})/dH$ of an isolated sublattice.[6] After averaging over azimuthal angles about the $\mathbf{n}$ axis, $\mathbf{M}_{\rm sl}(\mathbf{H},T)$ depends only on the angle $\theta = \arccos(\mathbf{n} \cdot \mathbf{m})$ between $\mathbf{n}$ and $\mathbf{H} = H\mathbf{m}$. Hence $\chi_{\rm sl}(\theta)$ can be expanded in Legendre polynomials $P_l(\cos\theta)$. Earlier work included $l = 0$, 1, and 2 polynomials.

A nonzero $l = 1$ term in the polynomial expansion implies that $\chi_{\rm sl}(0) \neq \chi_{\rm sl}(\pi)$. Hence the sublattice responds differently to a magnetic field along the $\mathbf{m} = \mathbf{n}$ ($\theta = 0$) and $\mathbf{m} = -\mathbf{n}$ ($\theta = \pi$) directions. But for a sublattice state with fixed $\mathbf{n}$, this asymmetry violates the Onsager relation,[10] which states that the diagonal components of the susceptibility tensor are invariant upon switching the orientation of the magnetic field. Onsager's relation implies that only even Legendre polynomials should contribute to the sublattice susceptibility.

Earlier work[6] suggested that the sublattice was more rigid for $\mathbf{H}$ along the $\mathbf{n}$ direction than along the $-\mathbf{n}$ direction. We believe that the asymmetric rigidity of the sublattice state arises from the way that one sublattice deforms the other. Because it is produced by the weak intersublattice coupling K_c, the sublattice deformation can be lifted by a weak magnetic field of order $K_c S/\mu_B \sim 1000$ Oe. Since the deformation of one sublattice by the other depends on their relative orientation, a term proportional to $\chi_0(1 - \mathbf{n}_1 \cdot \mathbf{n}_2)$ is added to the total sublattice susceptibility. If $\chi_0 > 0$, the sublattices are more easily deformed when $\mathbf{n}_1 = -\mathbf{n}_2$ (favored at low fields); if $\chi_0 < 0$, the sublattices are more easily deformed when $\mathbf{n}_1 = \mathbf{n}_2$ (favored at high fields).

The total susceptibility due to the deformation of the sublattices is then

$$\begin{aligned}\chi_{\rm def}(\mathbf{n}_1,\mathbf{n}_2;\mathbf{m}) = {} & 2\chi_0(1 - \mathbf{n}_1 \cdot \mathbf{n}_2) + 2\chi_1 \\ & + \chi_2\{\sin^2\theta_1 + \sin^2\theta_2\} \\ & + \chi_3\{\sin^4\theta_1 + \sin^4\theta_2\}, \end{aligned} \qquad (4)$$

where $\cos\theta_i = \mathbf{n}_i \cdot \mathbf{m}$ and the expansion in Legendre polynomials includes $l = 0$, 2, and 4 components. All coefficients χ_n are subject to the condition that $\chi_{\rm def}(\mathbf{n}_1,\mathbf{n}_2;\mathbf{m}) \geqslant 0$ for all orientations of $\mathbf{n}_1$ and $\mathbf{n}_2$.

For a cluster with sublattice orientations $\mathbf{n}_1$ and $\mathbf{n}_2$, the total magnetization is given by

$$\begin{aligned} 2\mu_B \mathbf{M}_{\rm clust}(\mathbf{n}_1,\mathbf{n}_2;\mathbf{m}) = {} & \mu_B M_{\rm sl} N_{\rm Cr}(\mathbf{n}_1 + \mathbf{n}_2) \\ & + \frac{N_{\rm Cr}}{2} H\mathbf{m}\, \chi_{\rm def}(\mathbf{n}_1,\mathbf{n}_2;\mathbf{m}). \end{aligned} \qquad (5)$$

Correspondingly, $-N_{\rm Cr}\, \chi_{\rm def}(\mathbf{n}_1,\mathbf{n}_2;\mathbf{m})H^2/4$ must be added to the energy of Eq. (3) for each cluster.

For a polycrystalline sample, the average magnetization is given by

$$2\mu_B M_{\rm av} = 2\mu_B \sum_i \int \frac{d\Omega}{4\pi} \langle \mathbf{M}_{\rm clust}(\mathbf{n}_{1i},\mathbf{n}_{2i};\mathbf{m}) \rangle \cdot \mathbf{m}, \qquad (6)$$

where we integrate over all orientations $\mathbf{m}$ of the external field and perform a thermal average over all orientations $\{\mathbf{n}_{1i},\mathbf{n}_{2i}\}$ in cluster i. Notice that $M_{\rm av}(T,H)$ depends on seven parameters: χ_n ($n = 0$, 1, 2, and 3), $M_{\rm sl}$, K_c, and $N_{\rm Cr}$. In the absence of the sublattice susceptibility, the average values for the saturation

magnetization would be given by $2\sqrt{3}\mu_B M_{\rm sl}$, $2\mu_B M_{\rm sl}$, and $2\sqrt{2}\mu_B M_{\rm sl}$ for cases (i), (ii), and (iii), respectively.

The fits based on this model break down close to $T_c \approx 33$ K and at high fields because the field-induced change in each sublattice moment becomes a substantial fraction of the zero-field moment. We shall employ a field cutoff of 3000 Oe and a maximum temperature of 30 K.

IV. AMBIENT PRESSURE

For each set of sublattice orientations $\mathbf{n}_i$, fits of the experimental magnetization at ambient pressure are presented in Figs. 2(a)–2(c). The quality of the fits is measured by

$$\sigma^2 = \frac{1}{N_d}\sum_i \left\{M_{\rm av}^{\rm expt}(H_i) - M_{\rm av}^{\rm th}(H_i)\right\}^2, \qquad (7)$$

where $M_{\rm av}^{\rm expt}(H)$ and $M_{\rm av}^{\rm th}(H)$ are the experimental and theoretical values for the average magnetizations at a fixed temperature and N_d are the number of experimental fields H_i. Since the energy E of Eq. (3) vanishes as $M_{\rm sl} \to 0$, the ratios of σ^2 for different cases must approach 1 as $T \to T_c$. Close to T_c, we expect that $\sigma^2({\rm ii})/\sigma^2({\rm i}) \sim 1 + \vartheta(M_{\rm sl}^2)$ and $\sigma^2({\rm iii})/\sigma^2({\rm i}) \sim 1 + \vartheta(M_{\rm sl}^2)$.

The ratios $\sigma^2/\sigma^2({\rm i})$ for cases (ii) and (iii) are plotted versus temperature in Fig. 1. Case (i) always provides the best fit with $\sigma^2({\rm ii})/\sigma^2({\rm i})$ and $\sigma^2({\rm iii})/\sigma^2({\rm i})$ reaching maxima at about 27 K. Above 27 K, the drop of both ratios is consistent with the reduction of $M_{\rm sl}$. For case (iii), the disagreement between the experimental data and the theoretical predictions is particularly egregious and can be clearly seen in Fig. 2(c) above 2000 Oe. The disparate quality of these fits supports our earlier claim that the sublattice moments lie along the cubic diagonals.

At least two factors are responsible for the sensitivity of the fits to the symmetry of the anisotropy axis. Due to the averaging over field direction in a polycrystalline sample, the external field is never precisely parallel to the net moment $\mathbf{n}_i$ of either sublattice. So even when $\chi_0 = \chi_1 = 0$, the sublattice susceptibility produces linear slopes of the average magnetization both at low fields and near saturation. Since both slopes sensitively depend on the symmetry of the anisotropy axis, it is difficult to simultaneously fit the magnetization data at low and high fields.

Just as importantly, the metamagnetic critical field H_c at low temperatures sensitively depends on the smallest angle between the external field and the anisotropy axis.[5] So the shape of the rise in the average magnetization near 1000 Oe is different for cases (i), (ii), and (iii). Taking these two factors together, the magnetization of a polycrystalline sample can be used to identify the symmetry of the anisotropy axis.

The resulting fitting parameters for case (i) (net sublattice spins along the cubic diagonals) are given in Fig. 3. In Fig. 3(a), K_c is roughly 5.2×10^{-3} meV at low temperatures and increases almost linearly with temperature above about 15 K. As expected, $M_{\rm sl}$ monotonically decreases with temperature in Fig. 3(a). The extrapolated value of $M_{\rm sl}(T=0) \approx 1.9$ is slightly smaller than the classical result $1.45S = 2.175$ derived earlier under the assumption of infinite anisotropy.

Both the correlation length ξ and $N_{\rm Cr} \sim \xi^3$ increase rapidly with temperature, as shown in Fig. 3(b). Results for $N_{\rm Cr}(T)$ can be fit by the critical scaling form $\xi(T) \propto (1 - T/T_c)^{-\nu}$ with an exponent $\nu \approx 1.1$, about twice the value $\nu = 0.5$ obtained in earlier work[5] and close to the value $\nu = 1$ for a two-dimensional Ising model.[11] Because of its unique properties, $Cr(Ru_2)_3$ may be the only known material where the magnetic correlation length ξ and critical exponent ν can be extracted directly from magnetization measurements

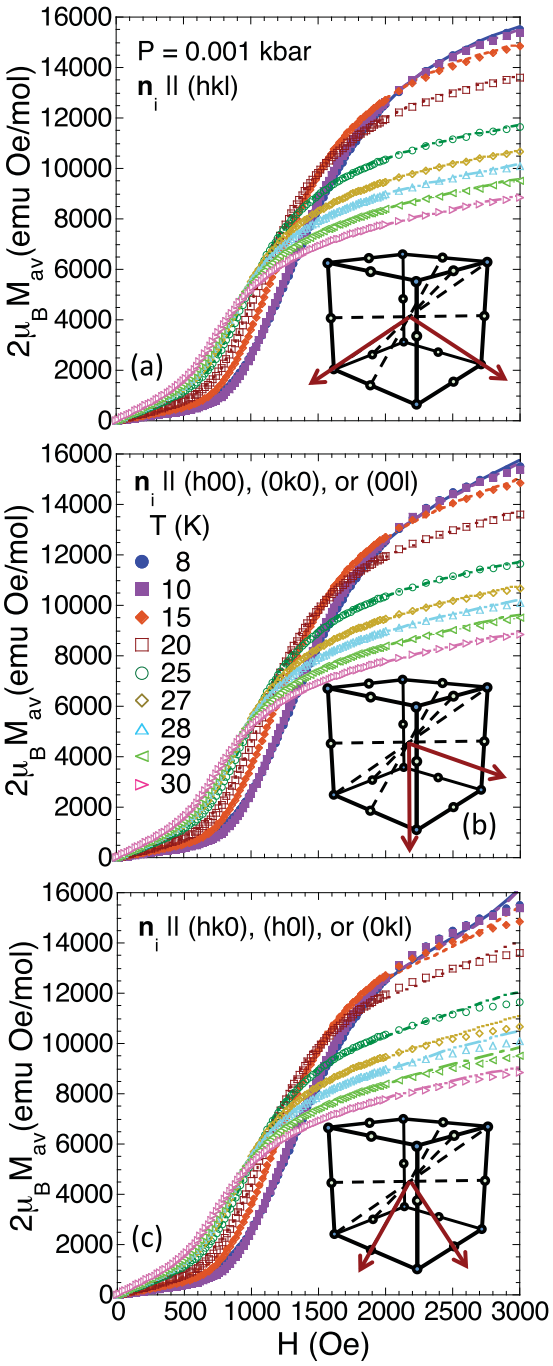

FIG. 2. (Color online) Fits for the average magnetization of a polycrystalline sample at ambient pressure (Ref. 7) with the sublattice moments restricted to (a) cubic diagonals, (b) cubic axis, or (c) edge diagonals with $h, k, l = \pm 1$. Insets show possible orientations $\mathbf{n}_i$ for the sublattice spins.

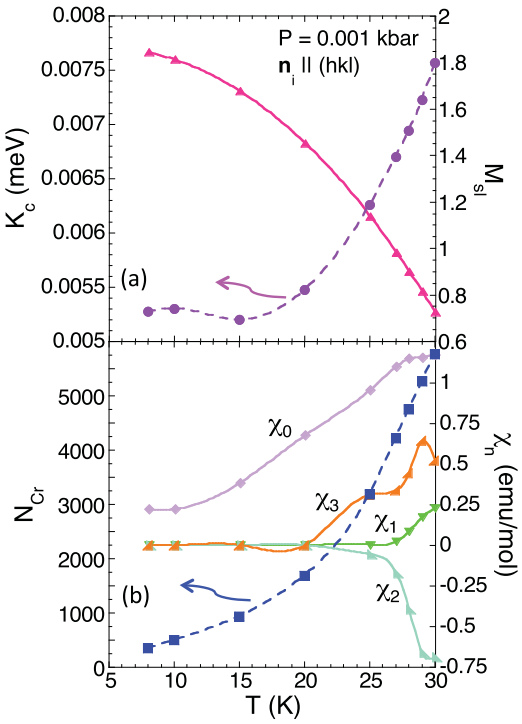

FIG. 3. (Color online) Fitting parameters versus temperature for $P = 0.001$ kbar and case (i): (a) intersublattice coupling K_c and sublattice spin M_{sl}, and (b) size N_{Cr} of a correlated magnetic cluster and sublattice susceptibility components χ_n.

rather than indirectly from internal probes like elastic neutron scattering.

Perhaps the deepest insight about the sublattice ground state is provided by the sublattice susceptibility components χ_n. The components χ_1, χ_2, and χ_3 reveal how each sublattice separately responds to a magnetic field oriented at an angle θ with respect to the spin $M_{sl}\mathbf{n}$. On the other hand, χ_0 reveals how one sublattice deforms the other. Our results plotted in Fig. 3(b) reveal that the sublattice susceptibility is dominated at low temperatures by χ_0. Since $\chi_0 > 0$, the sublattice deformation is greatest when the sublattices are aligned antiparallel. The rise of χ_0 with temperature implies that the sublattice deformation grows with temperature.

This surprising result answers a question left open by earlier work: Why are the two sublattices oppositely aligned in zero field? The dipolar interaction between two rigid sublattices favors *parallel* alignment with a coupling constant of approximately the same magnitude but opposite in sign to the one extracted from the magnetic susceptibility.[5] But K_c must include both the dipolar interaction between rigid sublattices (favoring parallel alignment) and the energy reduction due to the deformation of one sublattice by the other (favoring antiparallel alignment). Consequently, the rise of K_c with temperature in Fig. 3(a) may be related to the rise of χ_0 with temperature in Fig. 3(b).

V. PRESSURE DEPENDENCE

We recently speculated[6] that the pressure-induced phase transition in $Cr(Ru_2)_3$ at 7 kbar can be explained by a high-to low-spin transition[12] on the Ru_2 complex. With spin $S = 1/2$ on each Ru_2 complex, the net sublattice spin of the HP phase above 7 kbar would lie parallel to the Cr spins. Due to the reduced anisotropy on the Ru_2 complexes, the HP spin configuration would be more easily deformed by an external field.

But our earlier work did not permit a change in symmetry of the anisotropy axis with pressure. For example, the anisotropy axis might change from the cubic diagonals in the LP phase to the cubic axis in the HP phase. To resolve that issue, we have reanalyzed the magnetization curves under each of the three possible cases for the sublattice orientations. At 8 K and 11.68 kbar, $\sigma^2(\text{ii})/\sigma^2(\text{i}) \approx 3.8$ and $\sigma^2(\text{iii})/\sigma^2(\text{i}) \approx 9.4$. These smaller ratios are consistent with the suppressed value of M_{sl} in the HP phase. Hence the symmetry of the anisotropy axis does *not* change with pressure.

For case (i) (net sublattice spins along the cubic diagonals), the fits of the average magnetization remain quite good up to 12 kbar. Plotted in Fig. 4, the fitting parameters reveal a dramatic change at about 7 kbar. In Fig. 4(a), K_c jumps at the LP to HP transition, only to fall at higher pressures. As in earlier work,[6] the sublattice spin M_{sl} in Fig. 4(b) drops by roughly a factor of 2 from the LP to the HP phase. Below 7 kbar, N_{Cr} decreases with pressure in Fig. 4(b), indicating a reduction in the size of the fluctuating clusters. Possibly due to phase separation, N_{Cr} increases above 7 kbar.

As in ambient pressure, the susceptibility coefficients χ_n plotted in Fig. 4(b) provide a revealing signature of the sublattice spin state. Since $\chi_0 < 0$ above 7 kbar, the sublattices are more deformed when aligned parallel. Because

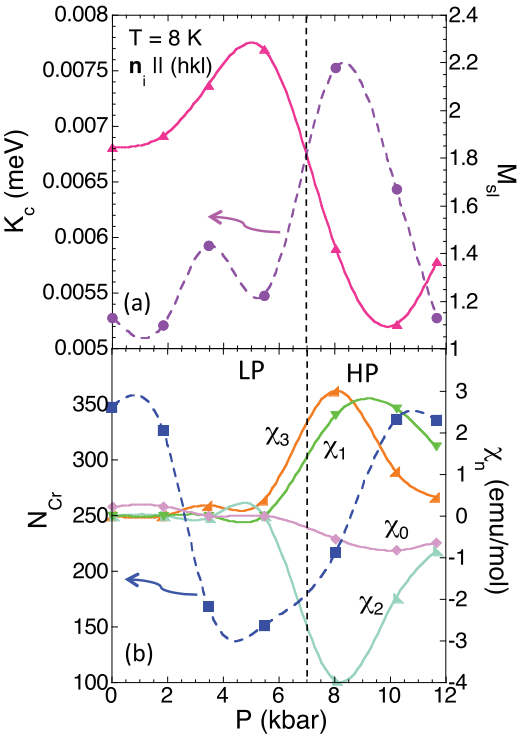

FIG. 4. (Color online) Fitting parameters versus pressure for $T = 8$ K and case (i): (a) inter-sublattice coupling K_c and sublattice spin M_{sl}, and (b) size N_{Cr} of a correlated magnetic cluster and sublattice susceptibility components χ_n.

the deformation energy favors parallel alignment, the dipolar interaction between rigid sublattices must favor antiparallel alignment in the HP phase.

Along with the drop in M_{sl}, the dramatic increase in the susceptibility components χ_1, χ_2, and χ_3 above 7 kbar provides convincing evidence for a LP to HP phase transition in $Cr(Ru_2)_3$. The larger value of χ_1 in the HP phase may be caused by the reduced anisotropy of the low-spin $S = 1/2$ Ru_2 moments.

VI. CONCLUSION

A remarkable amount of information can be extracted from the magnetization of a polycrystalline sample. Based on a simple phenomenological model and the varying quality of fits to experimental data, we have concluded that the sublattice moments of $Cr(Ru_2)_3$ are oriented along the cubic diagonals, in agreement with earlier predictions[5] for the sublattice ground state. A re-analysis of the susceptibility parameters as a function of pressure provides additional confirmation of a high- to low-spin transition on the Ru_2 complexes. Of course, future measurements are required to confirm this conjecture.

Ideally, the magnetic ground state of a molecule-based magnet would be determined from elastic neutron-scattering measurements on a deuterated single crystal. However, deuteration is quite expensive, single crystals are often difficult or impossible to obtain, and pressure-dependent measurements are even more challenging. While even neutron-scattering measurements on deuterated polycrystals can provide valuable information, those measurements are often difficult to interpret. In the absence of neutron-scattering results, we have demonstrated that a careful analysis of the average magnetization of a polycrystalline sample can provide important information about the magnetic ground state as a function of temperature and pressure.

ACKNOWLEDGMENTS

The original magnetization data were collected by William W. Shum and presented in Refs. 7 and 12. Useful conversations with Fernando Reboredo and Peter Stephens are also gratefully acknowledged. This research was sponsored by the Division of Materials Science and Engineering of the US Department of Energy (R.S.F.) and by the US National Science Foundation (Grant No. 0553573) (J.S.M.).

[1] Y. Liao, W. W. Shum, and J. S. Miller, J. Am. Chem. Soc. **124**, 9336 (2002).
[2] T. E. Vos, Y. Liao, W. W. Shum, J.-H. Her, P. W. Stephens, W. M. Reiff, and J. S. Miller, J. Am. Chem. Soc. **126**, 11630 (2004).
[3] T. E. Vos and J. S. Miller, Angew. Chem. **44**, 2416 (2005).
[4] J. S. Miller, T. E. Vos, and W. W. Shum, Adv. Mater. **17**, 2251 (2005).
[5] R. S. Fishman, S. Okamoto, W. W. Shum, and J. S. Miller, Phys. Rev. B **80**, 064401 (2009).
[6] R. S. Fishman, W. W. Shum, and J. S. Miller, Phys. Rev. B **81**, 172407 (2010).
[7] W. W. Shum, J. N. Schaller, and J. S. Miller, J. Phys. Chem. C **112**, 7936 (2008).
[8] V. M. Miskowiski, M. D. Hopkins, J. R. Winkler, and H. B. Gray, in *Inorganic Electronic Structure and Spectroscopy*, edited by E. I. Solomon and A. B. P. Lever (John Wiley & Sons, New York, 1999), Vol. 2, Chap. 6.
[9] W. W. Shum, Y. Liao, and J. S. Miller, J. Phys. Chem. A **108**, 7460 (2004).
[10] See, for example, R. M. White, *Quantum Theory of Magnetism* (Springer, Berlin, 2007), Sec. 1.3.3.
[11] See, for example, M. F. Collins, *Magnetic Critical Scattering* (Oxford University Press, New York, 1989).
[12] W. W. Shum, J.-H. Her, P. W. Stephens, Y. Lee, and J. S. Miller, Adv. Mater. **19**, 2910 (2007).